Astronomy & Astrophysics manuscript no. SFE_interactions
February 24, 2020

Gas fractions and depletion times in galaxies with different degrees of interaction

S. Díaz-García[1,2] and J. H. Knapen[1,2]

[1] Instituto de Astrofísica de Canarias, E-38205, La Laguna, Tenerife, Spain
e-mail: simondiazgar@gmail.com
[2] Departamento de Astrofísica, Universidad de La Laguna, E-38205, La Laguna, Tenerife, Spain

Received 20 Dec 2019 / Accepted 21 Feb 2020

ABSTRACT

Context. A moderate enhancement of the star formation rates (SFR) in local interacting galaxies has been reported, but the physical mechanisms leading to this increase are not clear.
Aims. We study the atomic gas content and the central stellar mass concentration for a sample of almost 1500 nearby galaxies to further investigate the nature of starbursts and the influence of galaxy-galaxy interactions on star formation.
Methods. We use the catalogue on interacting and merging galaxies in the S^{4}G survey of Knapen et al. (2014) along with archival H I gas masses, stellar masses (M_*), and SFRs (from *IRAS* far-IR fluxes), and calculate depletion times (τ) and gas fractions. We trace the central stellar mass concentration from the inner slope of the stellar component of the rotation curves, $d_R v_*(0)$.
Results. Starbursts – defined as galaxies with a factor > 4 enhanced SFR relative to a control sample (±0.2 dex in stellar mass, ±1 in T-type, non-interacting) – are mainly early-type ($T \lesssim 5$) massive spiral galaxies ($M_* \gtrsim 10^{10} M_\odot$), not necessarily interacting. For a given stellar mass bin, starbursts are characterised by lower gas depletion times, similar gas fractions, and larger central stellar mass concentrations than non-starburst galaxies. The global distributions of gas fraction and gas depletion time are not statistically different for interacting and non-interacting galaxies. However, in the case of currently merging galaxies, the median gas depletion time is a factor of 0.4 ± 0.2 that of control sample galaxies, and their star formation rates are a factor of 1.9 ± 0.5 enhanced, even though the median gas fraction is similar.
Conclusions. Starbursts present long-lasting star formation in the circumnuclear regions that causes an enhancement of the central stellar density at $z \approx 0$ in both interacting and non-interacting systems. Starbursts have low gas depletion timescales, yet similar gas fractions as normal main-sequence galaxies. Galaxy mergers cause a moderate enhancement of the star formation efficiency.

Key words. galaxies: starburst - galaxies: interactions - galaxies: spiral - galaxies: statistics

1. Introduction

There is plenty of observational work in the literature reporting a moderate statistical increase (by factor of a few) of the star formation rate (SFR) in interacting galaxies (e.g. Larson & Tinsley 1978; Bergvall et al. 2003; Smith et al. 2007; Woods & Geller 2007; Li et al. 2008; Robaina et al. 2009; Knapen & James 2009; Ellison et al. 2013; Barrera-Ballesteros et al. 2015; Brassington et al. 2015; Knapen et al. 2015). It is known that the most extreme starbursts, such as the ultraluminous infrared galaxies (ULIRGs), are almost always interacting or merging (e.g. Joseph & Wright 1985), and it is likely that the interaction has in fact stimulated the high SFR in such rare objects. The SFR enhancement has been found to be larger for smaller nuclear separation in galaxy pairs (Pan et al. 2019). However, Pearson et al. (2019) concluded that the SFR of merging galaxies is not significantly different from the SFR of non-merging ones, based on the use of convolutional neural networks applied to over 200000 galaxies. The astrophysics behind the SFR enhancement in interacting galaxies remains a matter of intense investigation.

An important ingredient for probing the link between SFR and interactions is the atomic and molecular gas content. Early work by Combes et al. (1994) reported an enhancement of the CO(1-0) luminosity, and also of the SFR, in tidally perturbed objects, indicating that the mass of molecular gas is higher in interacting systems. Using a sample of 107 visually classified post-merger galaxies, Ellison et al. (2018) found that merged galaxies exhibit an atomic gas fraction enhancement compared with the control sample (xGASS, Catinella et al. 2018) of the same stellar mass: they concluded that quenching is not a result of post-merger gas exhaustion (see also Pan et al. 2018). Lisenfeld et al. (2019) find no enhancement of the total H I+H_2 gas mass fraction in major-merger pairs, relative to non-interacting comparison samples. Larson et al. (2016) reported a dependence of the molecular gas mass fraction on the merger classification stage. They postulated that interactions sweep the available atomic hydrogen from the galaxy outskirts into the central regions, where it is converted into H_2 and, eventually, into newly formed stars. In this process, the encounter geometry is an important factor for the gas inflow, as shown in the simulations of Blumenthal & Barnes (2018). Analysis of interactions in the SIMBA cosmological simulation by Rodríguez Montero et al. (2019) reveals that major mergers (≤ 4:1) induce SFR enhancements due to an increase of the H_2 content at low masses, but when $M_* \geq 10^{10.5} M_\odot$ such an enhancement is attributed to a higher SF efficiency associated to denser gas.

This work aims at understanding in more detail why galaxies exhibit extreme values of SFR, whether they are interacting or not, expanding the work by Knapen et al. (2015) and Knapen & Cisternas (2015), using their sample of ∼ 1500 nearby galaxies drawn from the Spitzer Survey of Stellar Structure in Galaxies

(S^{4}G; Sheth et al. 2010). Without an anchoring of the analysis at cold gas masses, the desired comparison with theoretical predictions and simulations would remain incomplete. In this work we address this impediment using archival 21 cm H I integrated data. An additional goal is to shed light on the physical properties of the starburst galaxies, with emphasis on the central stellar mass concentration as well as their gas content.

2. Sample and data

Our parent sample is the S^{4}G, which is a magnitude- and diameter-limited survey that comprises 2352 galaxies with distances $\lesssim$ 40 Mpc observed in the 3.6 μm and 4.5 μm bands with the Infrared Array Camera (IRAC; Fazio et al. 2004) installed on-board the *Spitzer Space Telescope* (Werner et al. 2004).

Here, we use the catalogue of interacting and merging galaxies in the S^{4}G of Knapen et al. (2014). Our sample comprises 1341 galaxies. Of these, 16 are currently merging (class A), 39 appear highly distorted due to interaction with a companion (class B), and 84 present minor ongoing interaction (class C). The remaining 1202 galaxies constitute our control sample (CS) of non-interacting galaxies. We have excluded 138 galaxies from the Knapen et al. (2014) catalogue sample that belong to class "0", namely systems than have a close companion (within a radius of 5 times the diameter of the sample galaxy, recession velocity within ±200 km s^{-1}, and not more than 3 mag fainter) but show no signs of interaction.

The total star formation rates (SFR) used in this work are taken from Querejeta et al. (2015), who calculated them from the global *IRAS* photometry at 60 μm and 100 μm, following Larsen & Richtler (2000). Total stellar masses (M_*) are taken from Muñoz-Mateos et al. (2015) and are used to calculate specific star formation rates (sSFR=SFR/M_*). The same SFR values were applied by Knapen et al. (2015), who used M_* estimates from contaminant-free mass maps (Querejeta et al. 2015) derived from 3.6 and 4.5 μm imaging. Here we opt to consistently use the 3.6 μm passband for stellar mass inferences, including central concentration. Besides taking into account H I information, a further improvement with respect to the work by Knapen et al. (2015) is our use of the more refined morphological classifications by Buta et al. (2015), instead of those from HyperLEDA (Paturel et al. 2003). Atomic gas masses (in $M_\odot$) are estimated as (e.g. Giovanelli & Haynes 1988; Erwin 2018; Díaz-García et al. 2019b):

$$M_{\rm HI} = 2.356 \cdot 10^5 \cdot D^2 \cdot 10^{0.4\cdot(17.4-m21c)}, \quad (1)$$

where $m21c$ is the corrected 21-cm line flux in magnitude from HyperLEDA[1] (available for 98% of the galaxies in our sample) and D is the distance to the galaxy (in Megaparsec) adopted by Muñoz-Mateos et al. (2015). From this, gas depletion times (in yr) are calculated as (e.g. Knapen & James 2009):

$$\tau = \frac{2.3 \cdot M_{\rm HI}}{0.6 \cdot {\rm SFR}}, \quad (2)$$

where the factor 2.3 is applied to correct for helium and molecular gas content (Meurer et al. 2006), and the factor 0.6 accounts for the fraction of the formed stars which is recycled to the interstellar medium (James et al. 2008).

We also use the inner gradient of the stellar component of the rotation curve ($d_{\rm R}v_*(0)$, from Díaz-García et al. 2016b) as a proxy of the central stellar mass concentration (e.g. Erroz-Ferrer et al. 2016; Díaz-García et al. 2016a; Díaz-García et al. 2019a). Specifically, $d_{\rm R}v_*(0)$ was obtained from a polynomial fit to the inner part of disk+bulge component of the circular velocity, following Lelli et al. (2013), and taking the linear term as an estimate of the inner slope (80 of the 139 interacting and 768 of the 1202 non-interacting galaxies in our sample have reliable measurements of $d_{\rm R}v_*(0)$).

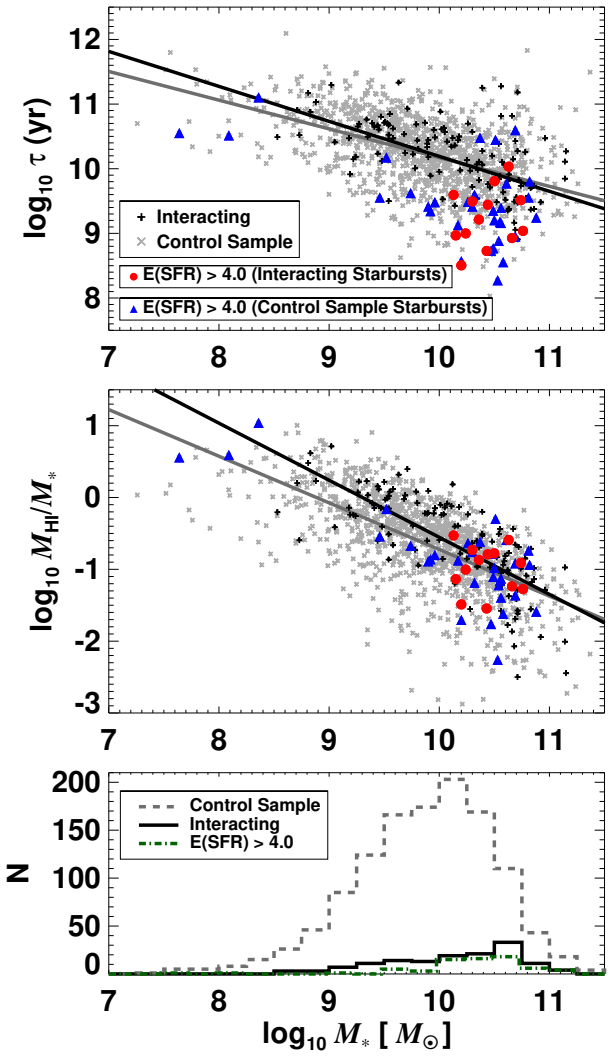

Fig. 1. Gas depletion time (*upper panel*) and gas fraction (*middle panel*) as a function of total stellar mass. (Non-) interacting galaxies, according to Knapen et al. (2014), are shown in (grey) black. (Non-) Interacting starbursts are shown in (blue) red, respectively (see legend). The lines correspond to the linear fit to the (non-)interacting galaxy points. In the *lower panel* we display the histogram of galaxies versus M_* (bins of 0.25 dex).

For every galaxy in our sample, we calculate the enhancement (E) in the global SFR, specific SFR, H I gas mass, gas fraction, and gas depletion time by dividing these parameters by the median values for a control sample: E(SFR)=SFR/<SFR>$_{\rm cs}$, E(sSFR)=sSFR/<sSFR>$_{\rm cs}$, $E(M_{\rm HI})=M_{\rm HI}/\langle M_{\rm HI}\rangle_{\rm cs}$, $E(M_{\rm HI}/M_*)=[M_{\rm HI}/M_*]/\langle M_{\rm HI}/M_*\rangle_{\rm cs}$, and $E(\tau)=\tau/\langle\tau\rangle_{\rm cs}$. A separate control sample is constructed for each individual galaxy, which encompasses all the non-interacting galaxies with similar values of T-type (±1) and total stellar mass (± 0.2 dex), following the criteria of Knapen et al.

[1] We acknowledge the usage of the database http://leda.univ-lyon1.fr

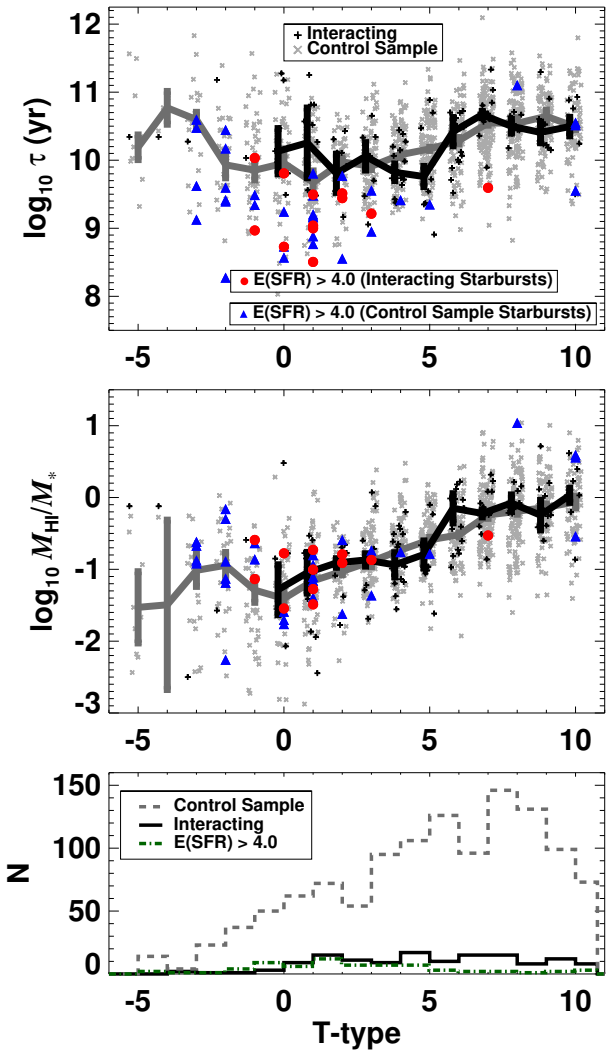

Fig. 2. As Fig. 1 but as a function of the revised Hubble stage. The running median (error bars obtained via bootstrap resamplings) are shown for interacting (black) and non-interacting (grey) galaxies separately. In the upper and central panels we have added small random offsets ($\lesssim 0.3$) to the T values in the $x-$axis (integers) to avoid point overlapping.

(2015). Whenever the control sample of a certain galaxy has less than 5 objects (47 cases), this galaxy is not included in our statistics. The median number of galaxies in the control samples is 46. In 17 cases (16 from CS, 2 of class A) with uncertain $T-$type, we selected the control sample based on M_* exclusively.

Starbursts are defined as those galaxies having E(SFR)> 4. Different SFR enhancement cutoffs (also on the sSFR) were tested by Knapen & Cisternas (2015, their Fig. 1), showing consistency in their result that the fraction of interacting galaxies is enhanced in starbursts. We checked and confirmed that the presented observational trends are qualitatively the same when starbursts are defined as E(SFR)$> 4-5$ or E(sSFR)$> 4-5$, fully in line with what Knapen & Cisternas (2015) reported.

3. Results

Depletion times and gas fractions decrease with increasing total stellar mass (Fig. 1). When studied in the Hubble sequence, τ and $M_{\rm HI}/M_*$ are larger for larger T among the spirals (Fig. 2). Curiously enough, τ seems to be larger than average among lenticulars, although the sampling of S0s is not optimal due to the bias of the S^{4}G towards late-type gas-rich systems.

For a given T- or M_*-bin, the average τ and $M_{\rm HI}/M_*$ are not significantly different for interacting and non-interacting galaxies (black and grey symbols and lines, respectively), as seen in both Fig. 1 and Fig. 2. To confirm this result, we performed a two-sample Kolmogorov-Smirnov (K-S) test (IDL implementation *kstwo.pro* written by W. Landsman, following Press et al. 1986), finding that the cumulative distribution function of τ and $M_{\rm HI}/M_*$ is similar for interacting and non-interacting galaxies, as indicated by the large (> 0.01) $p-$values (0.27 and 0.46, respectively).

The distribution of M_* for non-interacting galaxies peaks at $10^{10-10.25} M_\odot$ (lower panel of Fig. 1), while for interacting systems it peaks at slightly larger masses $M_* \approx 10^{10.5-10.75} M_\odot$. Interacting galaxies spread evenly across the Hubble sequence (lower panel of Fig. 2), but only 5 S0s in our sample are interacting. K-S tests indicate that the two arrays of M_* and T values for interacting and CS galaxies are drawn from different distributions ($p-$values of $3.8 \cdot 10^{-5}$ and $3.7 \cdot 10^{-3}$, respectively).

Fig. 3 shows the enhancements on SFR, H I gas mass and gas fraction (normalized by M_*), and gas depletion timescale for the different interaction classes. Median factors (and uncertainties obtained via bootstrap resamplings) are indicated at the top of the panels. The median enhancement in SFR (E(SFR)) increases with increasing degree of interaction, with class A presenting a median factor of 1.9 ± 0.5 higher SFR than the median for CS galaxies (in agreement with Knapen et al. 2015). Likewise, highly interacting systems are characterised by a median E(τ) of 0.4 ± 0.2. Regarding atomic gas masses, class B has median E($M_{\rm HI}$) and E($M_{\rm HI}/M_*$) of 1.9 ± 0.3 and 1.7 ± 0.3, respectively, but classes A and C do not show significant differences as compared to the CS. Extreme enhancements can be found in galaxies with different degrees of interaction or in complete isolation. Finally, enhancements on $M_{\rm HI}$, $M_{\rm HI}/M_*$, and τ are compared to that of the SFR in Fig. 4. E($M_{\rm HI}$) and E($M_{\rm HI}/M_*$) hardly show any correlation with E(SFR), as indicated by Spearman's correlation coefficients (significances) $\rho = 0.19$ ($p = 3.6 \cdot 10^{-12}$) and $\rho = 0.18$ ($p = 6 \cdot 10^{-11}$), respectively, while a more robust correlation between E(SFR) and E(τ) is found ($\rho - 0.45$, $p = 0$, naturally expected from the definition of τ).

There are 45 starburst galaxies in our sample, i.e. fulfilling E(SFR)>4. These are typically massive systems with $M_* \gtrsim 10^{10} M_\odot$ (Fig. 1) and Hubble stages $T \lesssim 5$ (Fig. 2) (80% of the cases). For a given M_*- or $T-$ bin, starbursts present lower gas depletion time scales than the median. However, their gas fractions are not larger than the median. This means that the lower τ is only determined by the enhanced SFR. There are three massive systems that, despite being starbursts, present high depletion timescales (NGC 2894, IC 2461, and UGC 07522): all three are S0$^-$ and S0^0 galaxies.

Starbursts are characterised by higher central concentrations of stars (Fig. 5): for a given M_*-bin, galaxies with E(SFR)> 4 show higher values of $d_{\rm R} v_*(0)$. Interacting and non-interacting galaxies are not significantly different in $d_{\rm R} v_*(0)$ for a certain M_*. However, as interacting galaxies are in general slightly more massive than their CS counterparts, their global $d_{\rm R} v_*(0)$ distribution peaks for slightly larger values, and thus the significance level of the K-S statistic between the subsamples of interacting and CS galaxies is fairly low ($p-$value of 0.0036).

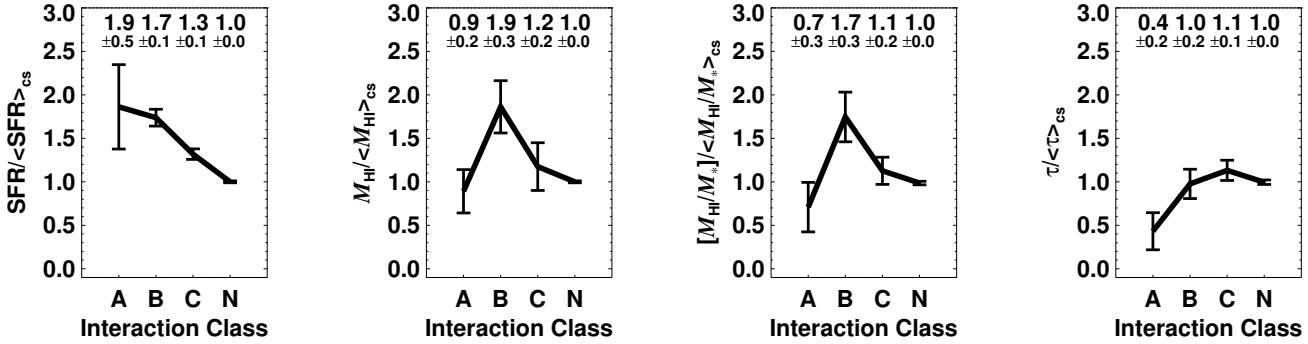

Fig. 3. Interaction class (A = merging, B = highly distorted due to interaction, C = minor interaction, N = control sample) versus SFR, gas mass, gas fraction, and depletion time, all normalised to CS median values (from left to right). We show the running median and the confidence limit based on bootstrap resamplings (values are displayed in the top, in red).

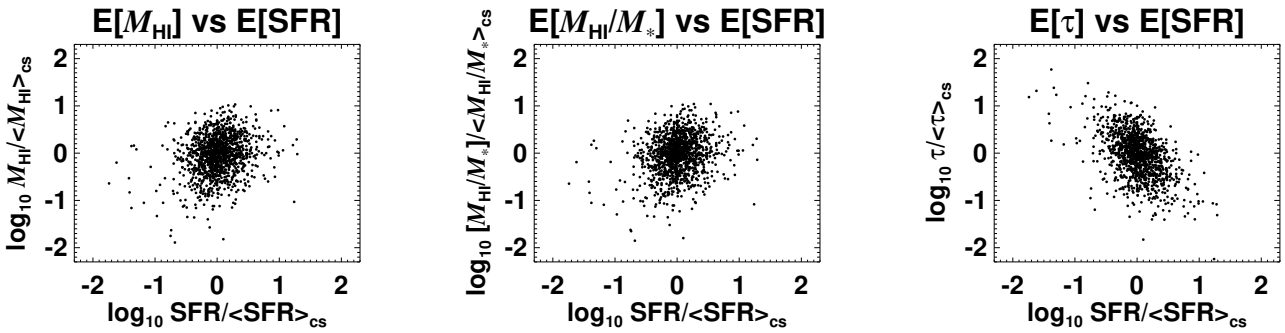

Fig. 4. Enhancement of H I gas masses (left), gas fractions (centre), and gas depletion times (right) as a function of enhancement on SFRs.

4. Discussion

Using refined morphological types (Buta et al. 2015) for the control sample definition, we confirm the result by Knapen et al. (2015) that the enhancement in SFR for highly interacting galaxies is a factor of ~ 2 higher than the average for CS galaxies. Our results are consistent with the expectations from the simulations by Di Matteo et al. (2007, 2008), who showed a similar enhancement of (circumnuclear) SF due to galaxy collisions, that drive the formation of non-axisymmetries that trigger inward gas flows (Barnes & Hernquist 1991; Mihos & Hernquist 1996).

In this work we take a step forward by adding the cold gas masses to the analysis for the different interacting classes. Studying separately all subclasses of interacting galaxies is undoubtedly insightful, yet uncertainties associated to the beamsize for the far-IR (*IRAS*) and 21 cm data (data from different telescopes are gathered in LEDA) may affect the measurements, and thus care must be taken to tone down conclusions based on interacting class. In certain cases (class A) strongly interacting galaxies may be so close that they could have been observed together, resulting in artificially increased values of $M_{\rm HI}$, SFR, or τ. We argue that such effects do not strongly affect our statistics when all interacting classes are grouped.

Knapen & James (2009) showed that H I total and relative mass are not strongly dependent on the absence or presence of a close companion, but do depend strongly on $T-$type. This is confirmed in this work with a four times larger sample (Fig. 2). Numerical models by Di Matteo et al. (2007) showed that the gas content in the merging event is not the main parameter governing the SF efficiency. Observational work by Violino et al. (2018) finds that gas fractions and depletion times in galaxy pairs are consistent with those of non-mergers whose SFRs are similarly raised. In addition, recent work by Ellison et al. (2018) shows that there is no correlation between a galaxy's H I gas fraction enhancement and its SFR enhancement (see their Fig. 7). We have assessed this in our sample and showed that, indeed, E(SFR) is barely correlated with E($M_{\rm HI}$) and E($M_{\rm HI}/M_*$) (Fig. 4).

Interestingly, we find that in highly distorted galaxies (class B) the H I mass is significantly enhanced (almost a factor of 2 higher than the CS, on average). This is not the case in class A, where the merger-driven enhanced SFR (plausibly prolonged for several Gyr) might have started to quench the galaxy, given the low depletion timescales. On the other hand, the cold gas could have been heated or removed via feedback from active galactic nuclei (e.g. Harrison et al. 2018; Ellison et al. 2019, and references therein). Also, Di Matteo et al. (2007) found that strong tidal interactions can remove a large amount of gas from the galaxy disks that is not fully re-acquired in the last merging phases. Finally, we note that the correlation between E(SFR) and E(τ) is not very tight (Fig. 4): this emphasises how controversial the definition of starburst can be (see Knapen & James 2009).

In interacting class A (mergers) we find the median τ to be a factor of 0.4 ± 0.2 that of the CS. This is consistent with the findings by Saintonge et al. (2012), who showed that among the gas-rich disk-dominated population galaxies those undergoing mergers or presenting disturbed morphologies are characterised by short depletion times, roughly a factor of two shorter when compared to the CS. Saintonge et al. also note that not all mergers or interactions are necessarily associated with episodes of efficient SF, as it is the case in our work: we also find low values of E(τ) among all interacting classes.

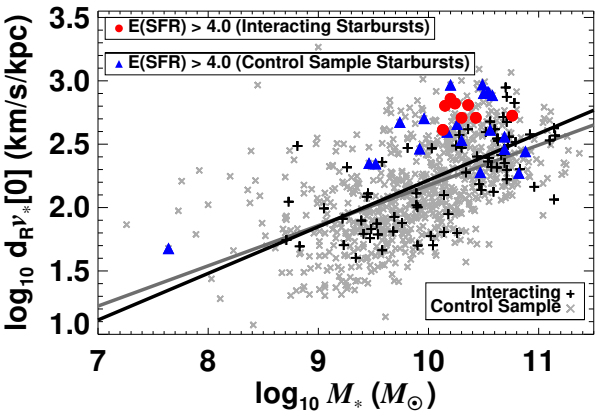

Fig. 5. Inner slope of the stellar component of the rotation curve (direct measurement of the central stellar mass concentration) versus total stellar mass for interacting (black) and non-interacting (grey) galaxies, while highlighting the starbursts (blue and red). The lines correspond to the linear fit to the data clouds.

Our analysis reveals that starbursts are characterised by a higher stellar mass central concentration when compared to a control sample, as measured from 3.6 μm imaging. This is most likely related to the fact that these galaxies mainly harbor newly formed stars in the circumnuclear regions at $z \approx 0$. This may imply that the SF enhancement is not associated with a single instantaneous central SF burst, but instead with either continuous SF over a period of 10^{8-9} yr (e.g. Knapen & James 2009), probably resulting from large-scale gas inflow driven by stellar non-axisymmetries, or a series of bursts over a significant timescale (e.g. Allard et al. 2006). In addition, gas depletion times are longer in bulge-dominated galaxies according to Saintonge et al. (2012). However, we have checked that the M_*-τ relation is not segregated as a function of $d_R v_*(0)$ (the bulge mass is larger for larger $d_R v_*(0)$, Díaz-García 2016). From SDSS-IV MaNGA data Pan et al. (2019) suggested that interaction-triggered SF is not necessarily limited to the circumnuclear regions, but the enhancement is centrally peaked. Recent work by Ellison et al. (2020) using MaNGA and ALMA data for 12 galaxies shows that an elevated SF efficiency is the fundamental driver for central starbursts, that are contributed by both interactions and secular mechanisms. In our work, high central stellar mass concentrations are detected for most starbursts regardless of whether they are interacting or not.

5. Summary and conclusions

We used a sample of 1341 S^{4}G galaxies from the catalogue on interacting and merging galaxies produced by Knapen et al. (2014) to analyse the effect of galaxy-galaxy interactions on star formation rates (SFR), atomic gas masses ($M_{\rm HI}$) and fractions ($M_{\rm HI}/M_*$), and depletions times (τ), using archival 21 cm H I data from HyperLEDA and *IRAS* far-IR fluxes (Querejeta et al. 2015). We also study the global physical properties of starburst galaxies, such as total stellar masses (M_*, from Muñoz-Mateos et al. 2015) and central concentration (traced from the inner slope of the stellar component of the rotation curves, $d_R v_*(0)$, using 3.6 μm imaging, from Díaz-García et al. 2016b). Starbursts are defined as galaxies having a factor > 4 enhanced SFR relative to a control sample, which comprises non-interacting systems having ±0.2 dex in M_* and ±1 in T (types from Buta et al. 2015). The main results of this paper are the following:

- We confirm that the distribution of gas fraction $M_{\rm HI}/M_*$ and depletion time τ is similar in interacting and control sample galaxies, but depends on M_* and T (e.g. Knapen & James 2009).
- In merging galaxies, the median enhancement in τ and SFR is a factor 0.4±0.2 and 1.9±0.5 that of the average for control sample galaxies, respectively (in line with earlier work by, e.g., Saintonge et al. 2012; Knapen et al. 2015).
- Highly distorted interacting galaxies have a factor of 1.9±0.3 enhanced H I mass. This is not the case in merging systems, where the (interaction-triggered) higher star formation efficiency might have started to quench the SF.
- Starbursts are typically early-type massive galaxies ($M_* \gtrsim 10^{10} M_\odot$, $T \lesssim 5$) and can be either interacting or non-interacting.
- For a given M_*-bin, starbursts present lower gas depletion time τ than the average, yet they have similar $M_{\rm HI}/M_*$. An enhancement of the SFR does not imply an enhancement of the relative and absolute amount of gas, or vice-versa.
- For a given M_*-bin, starbursts are characterised by higher central stellar concentrations. This points to these systems having undergone continuous circumnuclear star formation over a period of 10^8 to 10^9 yrs, nourished by gas inflow driven by both interactions and non-axisymmetries.

Acknowledgements. We thank the anonymous referee for comments that improved this paper. We acknowledge financial support from the European Union's Horizon 2020 research and innovation programme under Marie Skłodowska-Curie grant agreement No 721463 to the SUNDIAL ITN network, from the State Research Agency (AEI) of the Spanish Ministry of Science, Innovation and Universities (MCIU) and the European Regional Development Fund (FEDER) under the grant with reference AYA2016-76219-P, and from the IAC project P/300724 which is financed by the Ministry of Science, Innovation and Universities, through the State Budget and by the Canary Islands Department of Economy, Knowledge and Employment, through the Regional Budget of the Autonomous Community. JHK acknowledges financial support from the Fundación BBVA under its 2017 programme of assistance to scientific research groups, for the project "Using machine-learning techniques to drag galaxies from the noise in deep imaging". We thank Ute Lisenfeld for comments on the manuscript, and Miguel Querejeta for fruitful discussions. *Facilities*: *Spitzer* (IRAC).

References

Allard, E. L., Knapen, J. H., Peletier, R. F., & Sarzi, M. 2006, MNRAS, 371, 1087
Barnes, J. E. & Hernquist, L. E. 1991, ApJ, 370, L65
Barrera-Ballesteros, J. K., Sánchez, S. F., García-Lorenzo, B., et al. 2015, A&A, 579, A45
Bergvall, N., Laurikainen, E., & Aalto, S. 2003, A&A, 405, 31
Blumenthal, K. A. & Barnes, J. E. 2018, MNRAS, 479, 3952
Brassington, N. J., Zezas, A., Ashby, M. L. N., et al. 2015, ApJS, 218, 6
Buta, R. J., Sheth, K., Athanassoula, E., et al. 2015, ApJS, 217, 32
Catinella, B., Saintonge, A., Janowiecki, S., et al. 2018, MNRAS, 476, 875
Combes, F., Prugniel, P., Rampazzo, R., & Sulentic, J. W. 1994, A&A, 281, 725
Di Matteo, P., Bournaud, F., Martig, M., et al. 2008, A&A, 492, 31
Di Matteo, P., Combes, F., Melchior, A. L., & Semelin, B. 2007, A&A, 468, 61
Díaz-García, S. 2016, PhD thesis, University of Oulu
Díaz-García, S., Díaz-Suárez, S., Knapen, J. H., & Salo, H. 2019a, A&A, 625, A146
Díaz-García, S., Salo, H., Knapen, J. H., & Herrera-Endoqui, M. 2019b, A&A, 631, A94
Díaz-García, S., Salo, H., & Laurikainen, E. 2016a, A&A, 596, A84
Díaz-García, S., Salo, H., Laurikainen, E., & Herrera-Endoqui, M. 2016b, A&A, 587, A160
Ellison, S. L., Brown, T., Catinella, B., & Cortese, L. 2019, MNRAS, 482, 5694
Ellison, S. L., Catinella, B., & Cortese, L. 2018, MNRAS, 478, 3447
Ellison, S. L., Mendel, J. T., Patton, D. R., & Scudder, J. M. 2013, MNRAS, 435, 3627
Ellison, S. L., Thorp, M. D., Pan, H.-A., et al. 2020, MNRAS, 36

Erroz-Ferrer, S., Knapen, J. H., Leaman, R., et al. 2016, MNRAS, 458, 1199
Erwin, P. 2018, MNRAS, 474, 5372
Fazio, G. G., Hora, J. L., Allen, L. E., et al. 2004, ApJS, 154, 10
Giovanelli, R. & Haynes, M. P. 1988, Extragalactic neutral hydrogen., ed. K. I. Kellermann & G. L. Verschuur, 522–562
Harrison, C. M., Costa, T., Tadhunter, C. N., et al. 2018, Nature Astronomy, 2, 198
James, P. A., Prescott, M., & Baldry, I. K. 2008, A&A, 484, 703
Joseph, R. D. & Wright, G. S. 1985, MNRAS, 214, 87
Knapen, J. H. & Cisternas, M. 2015, ApJ, 807, L16
Knapen, J. H., Cisternas, M., & Querejeta, M. 2015, MNRAS, 454, 1742
Knapen, J. H., Erroz-Ferrer, S., Roa, J., et al. 2014, A&A, 569, A91
Knapen, J. H. & James, P. A. 2009, ApJ, 698, 1437
Larsen, S. S. & Richtler, T. 2000, A&A, 354, 836
Larson, K. L., Sanders, D. B., Barnes, J. E., et al. 2016, ApJ, 825, 128
Larson, R. B. & Tinsley, B. M. 1978, ApJ, 219, 46
Lelli, F., Fraternali, F., & Verheijen, M. 2013, MNRAS, 433, L30
Li, C., Kauffmann, G., Heckman, T. M., Jing, Y. P., & White, S. D. M. 2008, MNRAS, 385, 1903
Lisenfeld, U., Xu, C. K., Gao, Y., et al. 2019, A&A, 627, A107
Meurer, G. R., Hanish, D. J., Ferguson, H. C., et al. 2006, ApJS, 165, 307
Mihos, J. C. & Hernquist, L. 1996, ApJ, 464, 641
Muñoz-Mateos, J. C., Sheth, K., Regan, M., et al. 2015, ApJS, 219, 3
Pan, H.-A., Lin, L., Hsieh, B.-C., et al. 2019, ApJ, 881, 119
Pan, H.-A., Lin, L., Hsieh, B.-C., et al. 2018, ApJ, 868, 132
Paturel, G., Petit, C., Prugniel, P., et al. 2003, A&A, 412, 45
Pearson, W. J., Wang, L., Alpaslan, M., et al. 2019, A&A, 631, A51
Press, W. H., Flannery, B. P., & Teukolsky, S. A. 1986, Numerical recipes. The art of scientific computing
Querejeta, M., Meidt, S. E., Schinnerer, E., et al. 2015, ApJS, 219, 5
Robaina, A. R., Bell, E. F., Skelton, R. E., et al. 2009, ApJ, 704, 324
Rodríguez Montero, F., Davé, R., Wild, V., Anglés-Alcázar, D., & Narayanan, D. 2019, MNRAS, 490, 2139
Saintonge, A., Tacconi, L. J., Fabello, S., et al. 2012, ApJ, 758, 73
Sheth, K., Regan, M., Hinz, J. L., et al. 2010, PASP, 122, 1397
Smith, B. J., Struck, C., Hancock, M., et al. 2007, AJ, 133, 791
Violino, G., Ellison, S. L., Sargent, M., et al. 2018, MNRAS, 476, 2591
Werner, M. W., Roellig, T. L., Low, F. J., et al. 2004, ApJS, 154, 1
Woods, D. F. & Geller, M. J. 2007, AJ, 134, 527